Distamycin-NA: A DNA Analog with an Aromatic Heterocyclic Polyamide Backbone

Part 1

Synthesis and Structural Analysis of Monomers and Dimers Containing the Nucleobase Uracil

by **Guido Sauter**[1], **Eugen Stulz**, and **Christian Leumann***

Department of Chemistry and Biochemistry, University of Bern, Freiestrasse 3, CH-3012 Bern

The synthesis of the monomeric building block **13** and its constitutional isomer **12** of a new type of DNA analog, distamycin-NA, is presented (*Schemes 1* and *2*). This building block consists of a uracil base attached to a thiophene core unit *via* a biaryl-like axis. Next to the biaryl-like axis on the thiophene chromophore, a carboxy and an amino substituent are located allowing for oligomerization *via* peptide coupling. The proof of constitution and the conformational preferences about the biaryl-like axis were established by means of X-ray analyses of the corresponding nitro derivatives **10** and **11**. Thus, the uracil bases are propeller-twisted relative to the thiophene core, and bidentate H-bonds occur between two uracil bases in the crystals. The two amino-acid building blocks **12** and **13** were coupled to give the dimers **15** and **16** using dicyclohexylcarbodiimide (DCC) in THF/LiCl and DMF, respectively. While the dimer **15** showed no atropisomerism on the NMR time scale at room temperature, its isomer **16** occurred as distinct diastereoisomers due to the hindered rotation around its biaryl-like axis. Variable-temperature ^{1}H-NMR experiments allowed to determine a rotational barrier of 19 ± 1 kcal/mol in **16**. The experimental data were complemented by AM1 calculations.

1. Introduction. – Sequence-specific binding of single-stranded RNA and duplex DNA by synthetic DNA analogs is of general interest in medicinal chemistry [2]. Most of the analogs being investigated so far are structurally closely related to natural oligonucleotides, and only a few attempts to radically modify the backbone of DNA were successful. One of the most prominent candidates of the latter class are the peptide nucleic acids (PNA), first described by *Nielsen et al.* [3], in which the deoxyribose phosphate backbone of DNA was replaced by repeating *N*-(2-aminoethyl)glycine units to which the nucleobases were attached through a methylenecarbonyl linker. This DNA mimic recognizes RNA and DNA single strands selectively and with high affinity by the *Watson-Crick* base-pairing mode [4]. On the other hand, high-affinity, sequence-specific recognition of double-helical DNA is also mediated by small molecules. The antibiotics netropsin and distamycin, *e.g.*, are natural di- and tripeptides containing two and three 1-methyl-1*H*-pyrrole-2-carboxamide units, respectively [5]. The peptide chains of the antibiotics are crescent-shaped and preferentially recognize 4–5 sequential A · T base pairs in the minor groove of B-DNA by bifurcated H-bond formation. The recognition

[1]) Taken in part from the Ph.D. thesis of *G.S.* [1].

scheme can also be extended to longer sequence tracts by increasing the number of 1-methyl-1*H*-pyrrole units. A helical peptide that is a trimer of tetrakis (1-methyl-1*H*-pyrrole-2-carboxamide) coupled head-to-tail by *β*-alanine, synthesized by *Youngquist* and *Dervan* [6], was shown to bind one turn and a half of a DNA helix in a sequence-specific fashion. This demonstrates nicely that the inherent helicity induced by the pyrrole-substitution pattern matches the helical parameters of duplex DNA. To date, pyrrole-imidazole polyamides represent the only class of small molecules that bind any predetermined DNA sequence. Recent investigations by *Dervan* and coworkers showed that DNA recognition depends on side-by-side aromatic amino-acid pairings in the minor groove [7]. A pairing of imidazole (Im) opposite pyrrole (Py) targets a G · C base pair, and Py/Im targets a C · G base pair. A Py/Py combination is degenerate and targets both T · A and A · T base pairs.

In our design of the new DNA analog 'distamycin-NA', we wished to combine the elements of structural preorganization of the distamycin (crescent molecular shape) with the known complementary base-base recognition elements of the nucleic acids. It seemed attractive to connect a natural nucleobase, as a DNA recognition unit, *via* a biaryl-like bond to the position of a five-membered heterocycle lying between the amino and the carboxy group needed for chain extension (*Fig. 1*).

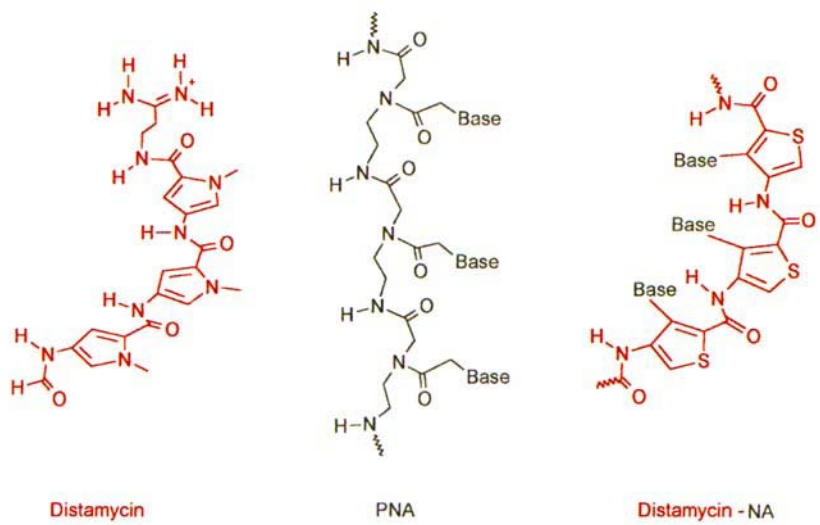

Fig. 1. *The blend of two characteristic structural concepts of DNA-binding polyamides* (distamycin and PNA) *leads to distamycin-NA*

This connection pattern forms a new interesting monomer unit in which putative backbone conformations are simply described by three torsion angles α, β, and γ (see **B** in *Fig. 2*) on the assumption that the interresidue amide bonds remain planar and *trans*-configured. DNA Recognition by distamycin-NA was examined with the aid of computer-assisted model building. According to this model, the base positions of the repetitive unit of distamycin-NA (see **B**) matches the bases in B-DNA (see **A**) if the

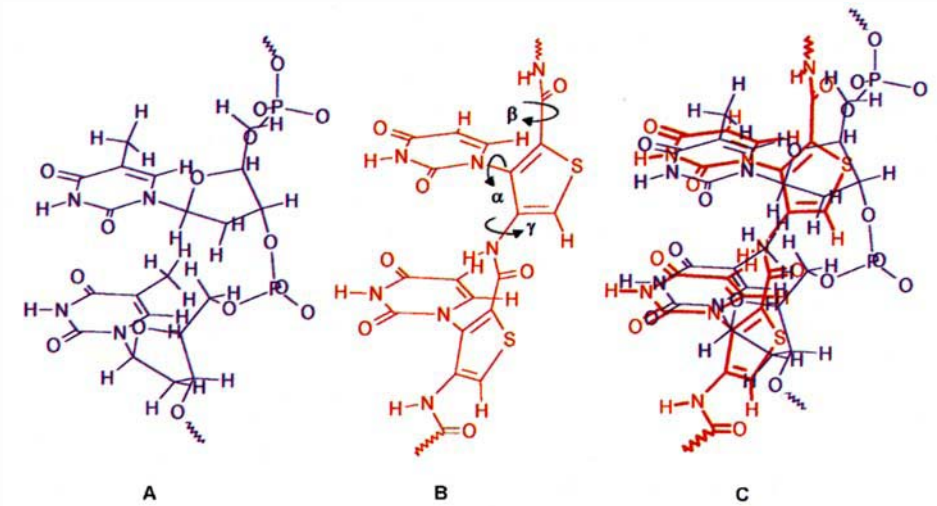

Fig. 2. *Modelled nucleobase positions of part of B-DNA* (**A**), *part of distamycin-NA* (**B**), *and overlay* (**C**) *of* **A** and **B**. By turning the three torsion angles α, β, and γ, one can find a repetitive unit of distamycin-NA in which its bases are superimposable with those of one strand in a B-DNA duplex.

torsion angles α, β, and γ adopt the values $\alpha = -121.08°$, $\beta = 121.29°$, and $\gamma = -90.0$, as can be seen from the overlay **C** of the two units **A** and **B** (*Fig. 2*).

We selected the heterocycle thiophene as the core unit because of the unique stability of its synthetic intermediates, compared to other analogous heterocycles as, *e.g.*, the pyrroles and furans. For the synthesis, we chose to use the known thiophene derivative methyl 3-(acetylamino)thiophene-2-carboxylate (**1**), used previously in biotin synthesis [8], as starting material. As already known, nitration of **1** leads to the two separable isomers **2** and **3**. While the isomer **3** showed the desired substitution pattern of the heterocycle, its isomer **2** served as a welcome additional compound for the study of the structural properties of the biaryl-like axis in such systems. For the choice of the recognition moiety in the repetitive monomer unit, the nucleobase uracil was selected because of the known straightforward procedures of its preparation.

Here we describe the synthesis of two types of monomers and dimers containing the base uracil, its structural analysis by X-ray and variable-temperature NMR spectroscopy, as well as a theoretical conformational analysis by AM1 calculations.

2. Results and Discussion. – 2.1. *Synthesis of Monomers.* Our synthesis of the monomeric building blocks started from the already known thiophene derivative **1** which was nitrated with H_2SO_4/HNO_3 at $-25°$ (*Scheme 1*). The resulting mixture of the isomers **2**/**3** were separated by fractionated crystallization from toluene[2]). Deacetylation of **3** with NaOMe in MeOH at 60° afforded **5** in 80% yield. Under similar conditions, **4** could only be obtained in 62% yield from **2**, probably due to partial polymerization.

---

[2]) According to *Vogel*, *Rossy*, and coworkers [8], the structures were identified and assigned on the basis of their melting points. It has been pointed out later by *Elliott et al.* [11] that this assignment was wrong. We can confirm the corrections provided by the latter authors.

Scheme 1

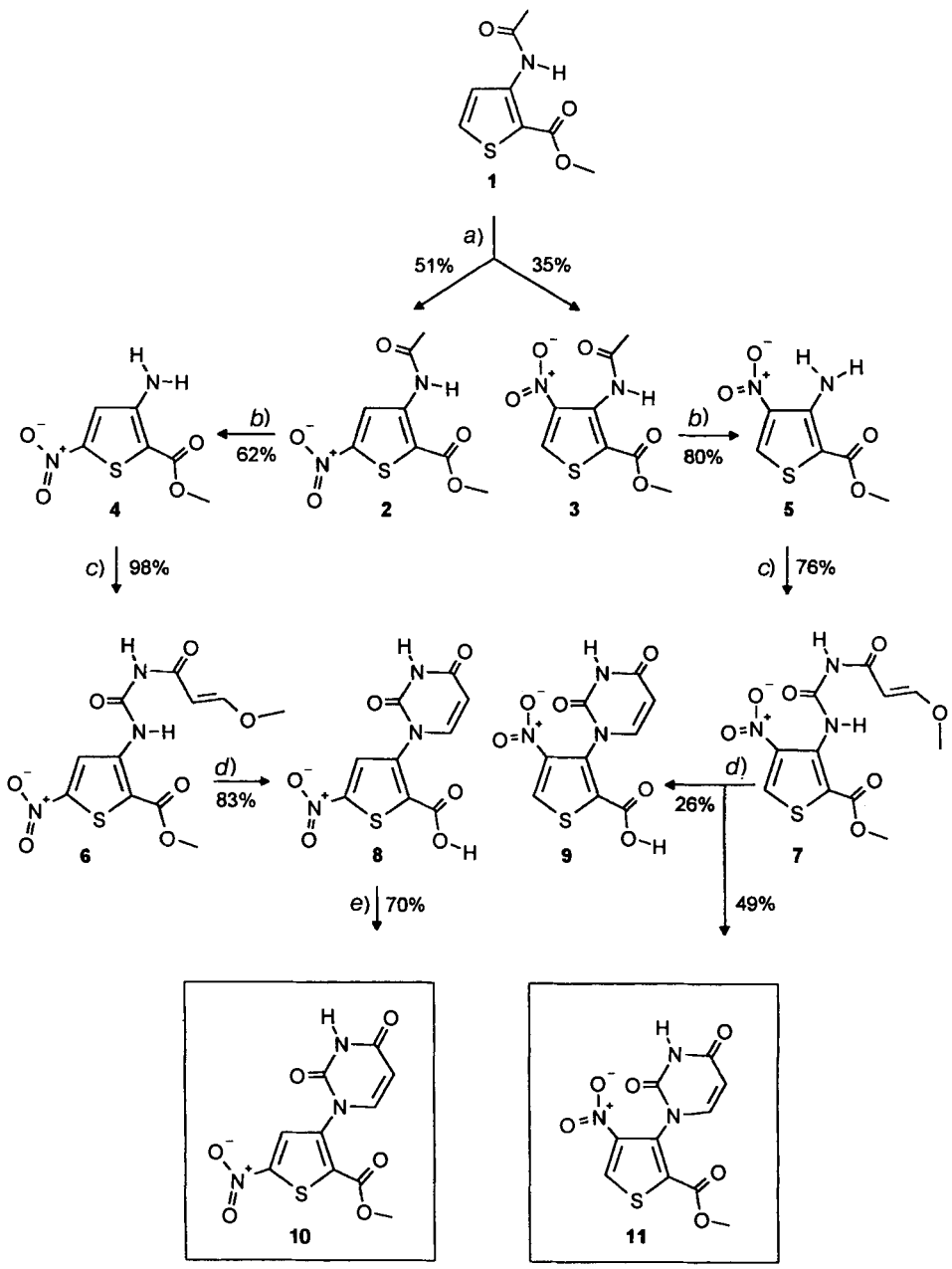

a) H_2SO_4/HNO_3, 45 min, −25°. *b*) MeOH/NaOMe, 0.5–1 h, 60°. *c*) MeOCH=CHCONCO, DMF/Et_2O 3:1, 1.5–2.5 h, −10°, 3.5–10 h, 4–25°. *d*) 2M H_2SO_4, 1.75–12.75 h, reflux. *e*) MeOH/BF_3OEt_2, 72 h, reflux.

Both isomers **4** and **5** were converted into the corresponding uracil derivatives in analogy to procedures by *Shaw* and *Warrener* [9] and *Shealy et al.* [10]. Starting from the commercially available methyl 3-methoxyacrylate, we generated the highly reactive 3-methoxyacryloyl isocyanate which was subsequently added to the amines **4** and **5** producing the ureas **6** and **7**, respectively. Pure **6** was obtained in 80–98% yield after precipitation, while its isomer **7**, isolated in 76% yield after extractive workup, was contaminated with *ca.* 4% (^{1}H-NMR) of 3-methoxyacrylic acid. However, **7** was used subsequently without further purification. The ring closure of urea **7** to the uracil derivative **11** was achieved in 49% yield by refluxing in 2M H_2SO_4; it was acompanied by acid-catalyzed ester hydrolysis producing also acid **9** (26% yield). When urea **6** was treated in the same manner, acid **8** was obtained as the major product besides only traces of the ester **10**. In contrast to the ring-closure reaction of **7**, urea **6** needed much longer refluxing to effect condensation. Thus, due to the harsher condensation conditions, only acid **8** could finally be isolated (83%). Subsequently, **8** was transformed in 70% yield into **10** by treatment with MeOH and $BF_3 \cdot Et_2O$ according to the procedure of *Kadaba* [12].

2.2. *X-Ray Structures of Monomers* **10** *and* **11**. To obtain additional proof for the constitution and to get insight into the conformational preferences of the monomers **10** and **11**, X-ray analyses were performed (*Figs. 3* and *4*). Crystals suitable for X-ray structure analysis could be obtained by letting saturated solutions of **10** and **11** in CH_2Cl_2/MeOH/benzene 5:1.5:0.2 slowly evaporate at room temperature over several days.

The thiophene unit in **10** forms a typical distorted five-membered ring showing high double-bond character for the bonds C(4′)–C(5′) and C(2′)–C(3′) and a high single-bond character for the C(3′)–C(4′), S(1′)–C(2′), and S(1′)–C(5′) bonds, as well as a small bond angle C(5′)–S(1′)–C(2′) of 89.52°. These are known to be general features of thiophene derivatives [13]. A comparison of the observed bond and angle values of the uracil base with known literature values shows also no relevant differences for this structural subunit [14]. The three substituents of the thiophene ring, the nitro function, the COOMe group, and the uracil ring form planes that are propeller-twisted relative to the thiophene plane. The interplanar angle between the uracil and thiophene moieties corresponding to the torsion angle α is 46.8° (*Table 1*). The atoms of the uracil and thiophene unit deviate slightly from planarity. The maximal observed deviation from the idealized calculated planes is 0.014 Å. The two planes containing the nitro and ester function are almost coplanar to the thiophene core. The bonds C(5′)–N(6′) and C(2′)–C(9′), however, show only weak double-bond character. The carbonyl group (C(9′)–O(10′)) is located *trans* relative to the thiophene ring.

The crystallographic repetitive unit of **10** contains four symmetry-adapted molecules. The base and thiophene units are stacked along the crystallographic *a* axis. The distance between the planes of stacked thiophene and base units is 3.905 Å. In the crystal, intermolecular contacts occur between neighboring uracil units. They form bidentate base pairs connected by two H-bonds N(3)–H ··· O(4). The distance between the heteroatoms is 2.814 Å. Chirality is induced by the non-planarity of the aromatic residue. Therefore, in the crystal, a racemate containing *P*- and *M*-enantiomers is observed (*Fig. 3*).

In the case of the isomer **11**, the geometries (bond angles and length) of the uracil and thiophene units are similar as described for **10**. The atoms of the base and the thiophene

a)

Selected torsion angles

α: C(2)-N(1)-C(3')-C(2') **223.00°**
β: C(3')-C(2')-C(9')-O(11') **191.44°**
γ: C(4')-C(5')-N(6')-O(8') **-0.67°**

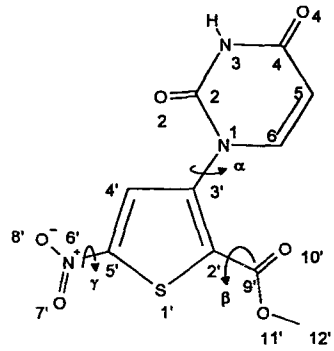

b)

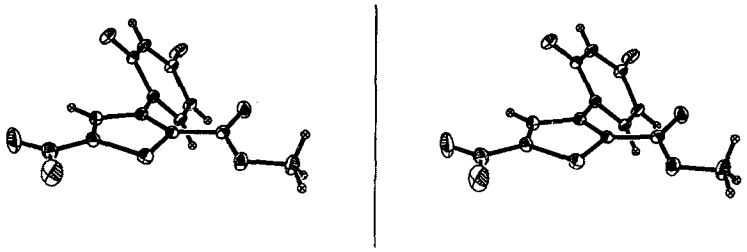

c)

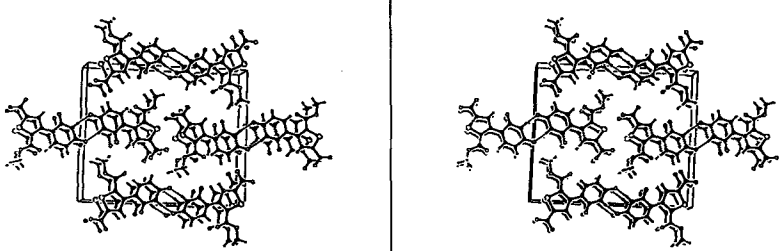

Fig. 3. a) *Molecular structure of* **10** *showing atom numbering* (arbitrary) *and selected torsion angles.* b) *Stereo ORTEP representation of* **10** (displacement ellipsoids are drawn at 50% probability). c) *Stereo representation of the packing diagram of* **10**. H-Bonds are shown as dashed lines.

deviate maximally by 0.008 Å from the idealized planes. As in the case before, **11** crystallizes as a racemate with *P*- and *M*-enantiomers connected through bidentate uracil pairs (two N(3)–H···O(4) bonds). The base pairs form axial helical repeating ribbons (*Fig. 4*). Selected torsion angles and minimal interplanar angles are given in *Fig. 4* and *Table 1*.

a)

Selected torsion angles

α: C(2)-N(1)-C(3')-C(2')	**87.17°**
β: C(3')-C(2')-C(9')-O(11')	**172.74°**
γ: C(5')-C(4')-N(6')-O(7')	**2.05°**

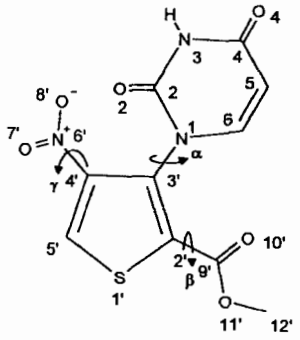

b)

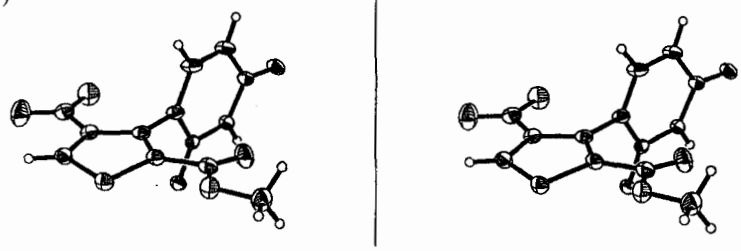

c)

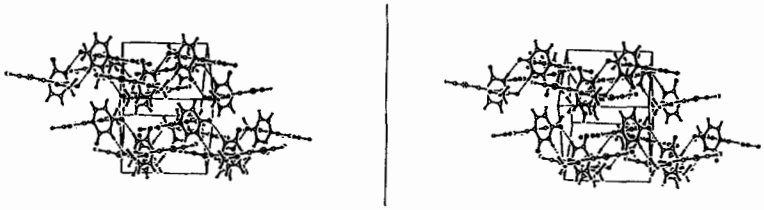

Fig. 4. a) *Molecular structure of* **11** *showing atomic numbering* (arbitary) *and selected torsion angles.* b) *Stereo ORTEP representation of* **11** (displacement ellipsoids are drawn at 50% probability). c) *Stereo representation of the packing diagram of* **11**. H-Bonds are shown as dashed lines.

Table 1. *Interplanar Angles between the Idealized Planes Formed by the Thiophene Core and the Uracil Base, the Ester Group or the Nitro Substituent*

Minimal interplanar angle between	Structure **10**	Structure **11**	Difference of angle between **10** and **11**
Uracil/thiophene	46.84°	89.59°	42.75°
Ester/thiophene	14.62°	8.05°	−6.57°
Nitro/thiophene	2.29°	1.80°	−0.49°

The main structural difference between **10** and **11** lies in the torsion angle α. The biaryl-like axes of **11**, in contrast to **10**, has two demanding substituents as neighbors leading to a higher degree of propeller-twisting of the heterocyclic planes due to release of steric strain. Interestingly, in both isomers **10** and **11**, the other rotational axis (β and γ) are hardly twisted. The observed interplanar angles between the nitro group and the thiophene core as well as the ester group and the thiophene core are between 1.8 and 2.3°, and 8.1 and 14.6°, respectively (*Table 1*). A search in the *Cambridge Structural Database* for structures consisting of an *ortho*-disubstituted five-membered aromatic heterocycle connected to a six-membered heterocycle with one *ortho*-substituent *via* a biaryl-like axis yielded no entries.

2.3. *Synthesis of Dimers.* Preliminary experiments for the reduction of the nitro function in **10** and **11** were performed on the isomer **10**. Reduction with Zn dust in $MeOH/NH_4Cl$ yielded air-sensitive Zn^{2+} complexes. After removing the Zn^{2+} with sat. EDTA/sat. $NaHCO_3$ solution 1:1, the amine **12** could be isolated in variable yields from 5 to 60%. The variable and low yields were mostly due to the difficulties encountered in the extractive workup. The product was hardly soluble in organic solvents, and continuous extraction with a perforator was impossible because of the temperature sensitivity of the [Zn^{II}(thiophene)] complexes. Reduction in analogy to the *Zinin* procedure [15] (NaHS in aqueous MeOH or THF) was found to be unsuccessful, too; besides unidentified water-soluble by-products, amine **12** could only be isolated in up to 30% yield.

The reduction method of choice for both nitro isomers was found in the catalytic hydrogenation. Treatment of **10** and **11** with H_2 over 10% Pd/C in THF/AcOH 5:1 afforded the amines **12** and **13** in 80 and 77%, respectively (*Scheme 2*). The addition of AcOH inhibited the formation of by-products originating from incompletely reduced nitro derivatives. On the other hand, acetylation (3–10%) of amine **13** to acetyl derivative **14** had to be taken into account, a reaction absent in the case of **12**. The observed preferred acetylation of **13** can be explained by the higher nucleophilicity of the amino group in **13** relative to **12**, the latter showing the characteristics of a doubly vinylogous amide.

Coupling of the acyl chloride generated from **8** (treatment with oxalyl chloride) and of amine **12** in MeCN/pyridine yielded, after chromatographic purification and ion exchange[3]), only 20% of dimer **15**. At first, coupling attempts with DCC in CH_2Cl_2 or MeCN failed, probably due to the low solubility of the starting material. Inspired by the work of *Seebach* and coworkers [16], describing the higher solubility of peptides in THF/LiCl mixtures, we tried the coupling of **8** and **12** with DCC in THF/LiCl (25 equiv. per monomer unit **12**). After 2–3 h reaction time, 66% of dimer **15** could be isolated (*Scheme 2*). The same method failed to generate the isomeric dimer **16** from **9** and **13**. However, coupling with DCC/BtOH in DMF was successful, and after 24 h, 59% of dimer **16** were isolated.

2.4. *Structural Analysis of Dimers.* At room temperature, the ^{1}H-NMR of **15** shows only resonances originating from one atropisomeric form, whereas that of **16** exhibits in

---

[3]) Treatment with *Amberlyst 15* (H^+ form, THF/H_2O 2:1) was necessary because, after chromatography (silica gel, MeOH/CH_2Cl_2/Et_3N 1:10:0.05 and EtOH/CH_2Cl_2/Et_3N 2:8:0.05), **15** was isolated in its Et_3NH^+ form (deprotonated at the interresidue amide N-atom) as determined by ^{1}H-NMR.

Scheme 2

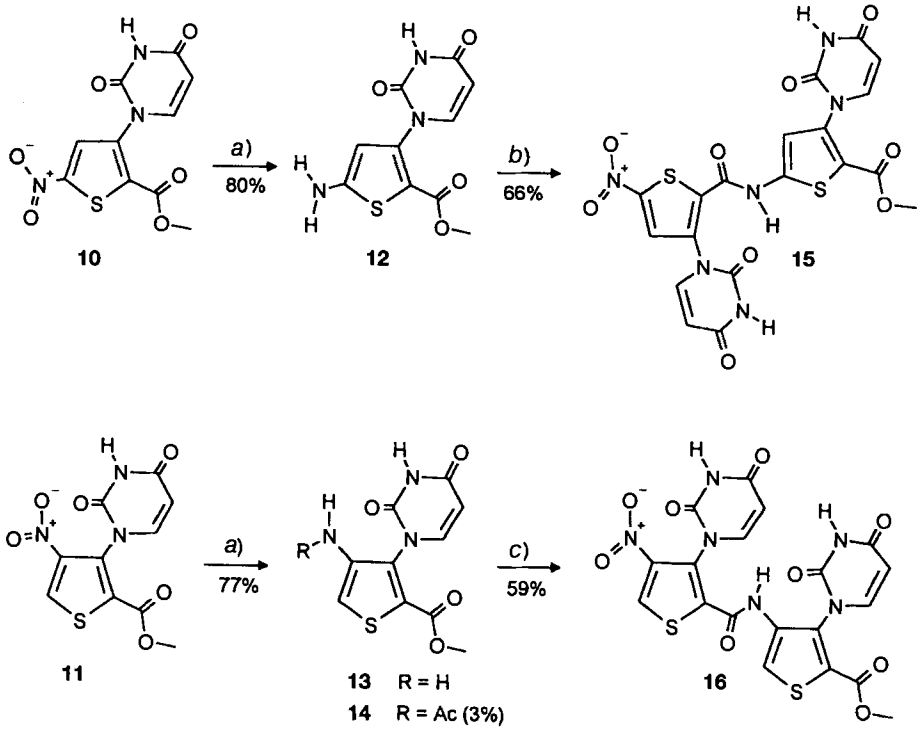

a) H_2, 10% Pd/C, THF/AcOH 5:1, 1–18 h. *b*) **8**, DCC, THF/LiCl, 2.5 h. *c*) **9**, DCC/BtOH, DMF, 24 h.

the aromatic region a doubled set of resonances attributed to two atropisomeric forms that are stable on the NMR time scale (*Fig. 5*).

In the ^{1}H-NMR spectrum of **15** at room temperature (*Fig. 5,a*), the two resonances of H–C(5)(y^1) and H–C(5)(y^2), which couple with 8 Hz to the signals of H–C(6)(y^1) and H–C(6)(y^2) at 7.81 and 7.60 ppm, respectively, as well as with 2 Hz to the signals of H–N(3)(y^1) and H–N(3)(y^2), respectively, are located at 5.76 and 5.65 ppm. Between the two base signals, the signal of H–C(4′)(y^2) is located at 7.03 ppm. In contrast, the ^{1}H-NMR spectrum of **16** shows in the same region at room temperature doubled signals for H–C(5), H–C(6), and H–C(5′) in a ratio of *ca.* 1:1 (*Fig. 5,b*).

To determine the rotational barrier in **16**, variable-temperature ^{1}H-NMR experiments (*Fig. 6*) were performed. By raising the temperature, signal coalescences followed by the development of sharper signals were observed, indicating that the life-time of the initial rotamers of **16** decreased at higher temperatures. These experiments and also further ^{13}C-NMR experiments (not shown) strongly supported the hypothesis of a substantial rotational barrier around one of the biaryl-like axis. In *Table 2*, the extrapolated temperatures of coalescence T_c and the differences of frequencies $\Delta\nu$ at room temperature are given. With these data, a rotational barrier of 19 ± 1 kcal/mol was calculated using the approximation described in [17]. Similar values of rotational barriers were observed by *Içli* [18] in structurally related axially chiral compounds that feature two sp^2-hybridized atoms linked by a single bond.

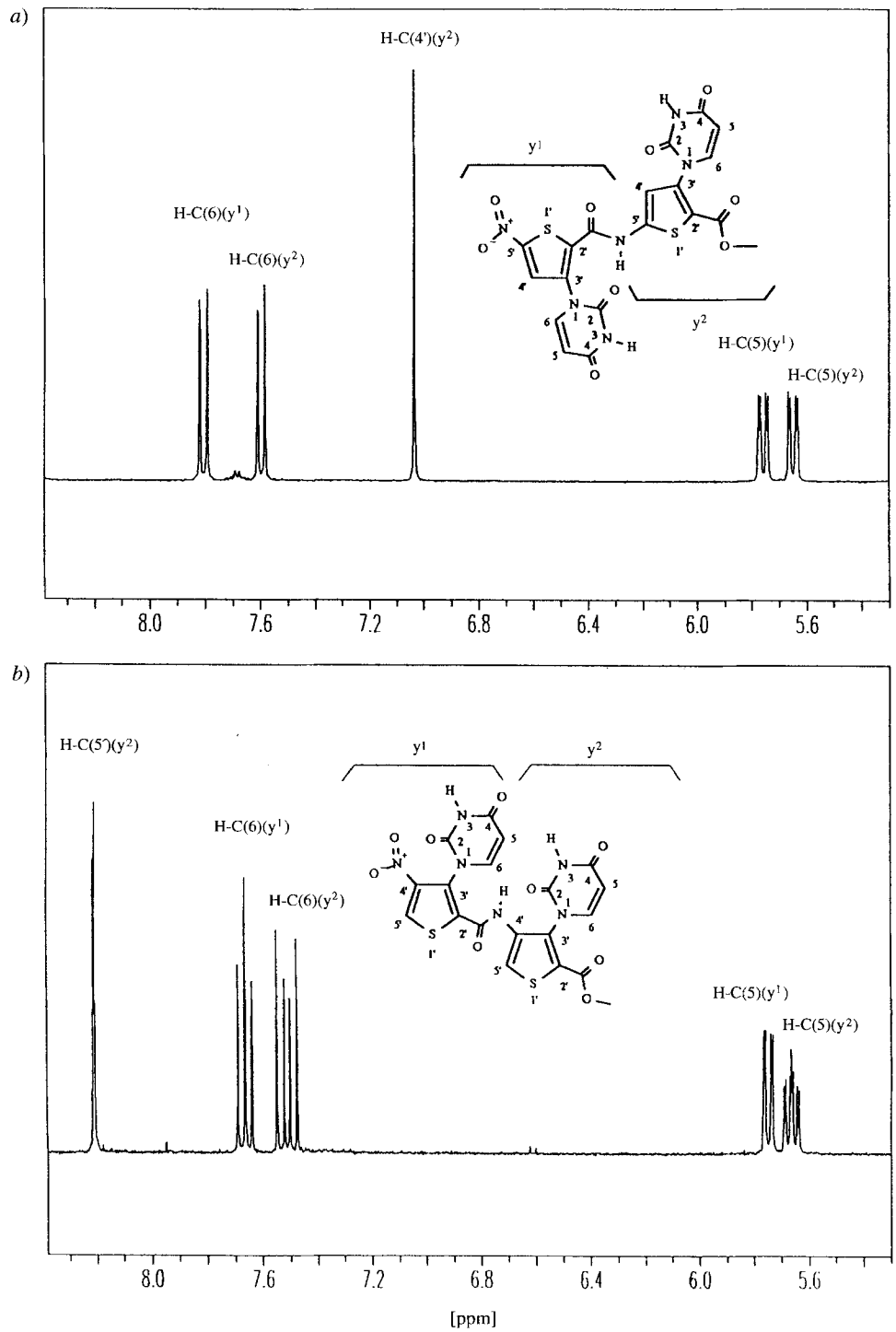

Fig. 5. *Section of ^{1}H-NMR spectra* (300 MHz, (D_6)DMSO, r.t.) *of the aromatic protons of* a) **15** *and* b) **16**. Arbitrary numbering. The aromatic region shows clearly one set of resonance signals for **15** and two sets for **16** indicating the presence of two atropisomeric forms in the latter compound.

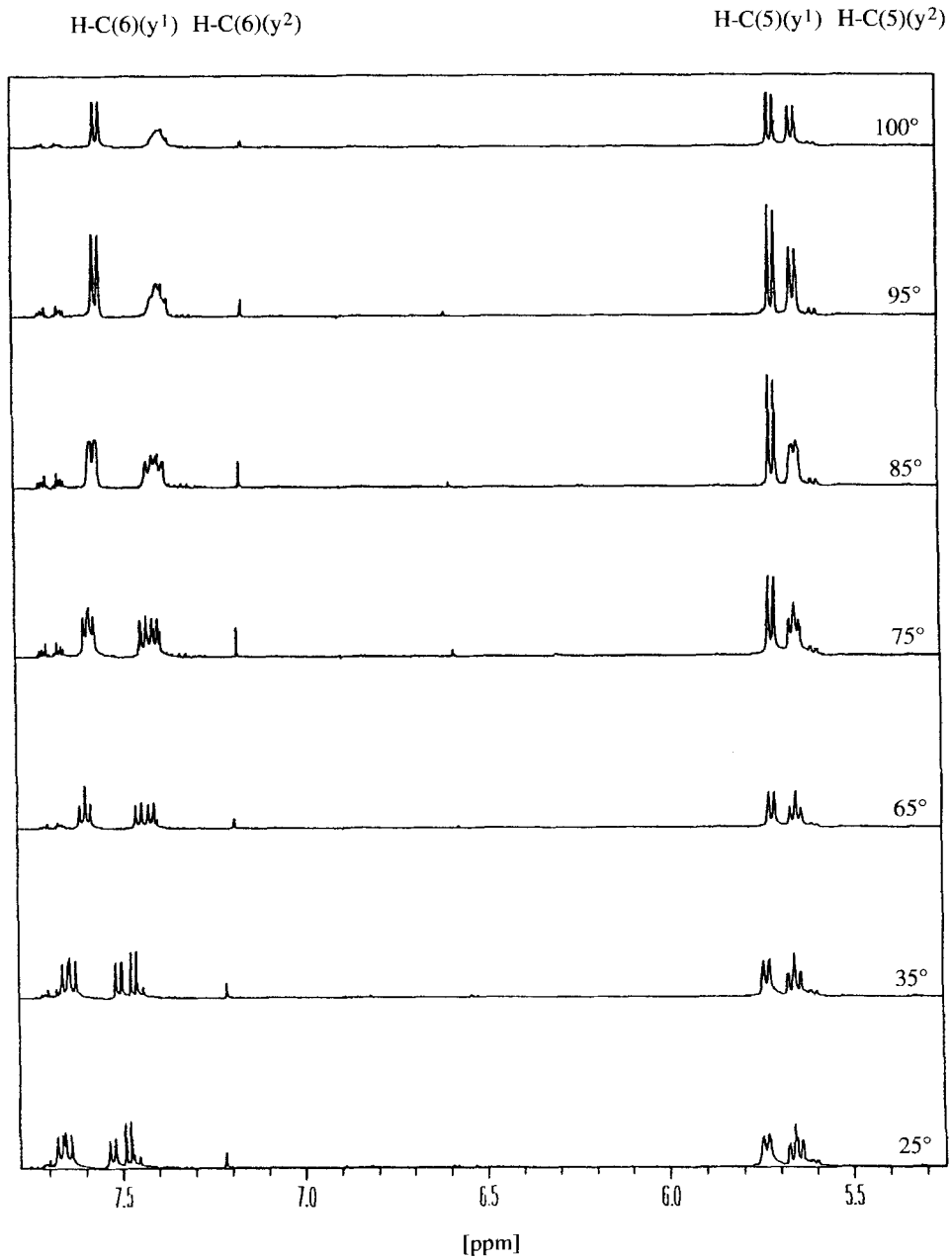

Fig. 6. *Section of* ^{1}*H-NMR spectra* (500 MHz, (D_6)DMSO) *of* **16** *at different temperatures.* For numbering, see *Fig. 5.*

Table 2. *Determination of the Rotational Barrier between the Two Atropisomeric Forms of* **16**

Signal[a])	T_c [°C][b])	$\Delta\nu$ [Hz][c])	ΔG^* [kcal/mol][d])
H–C(5)(y^2)	85	6.62	19.0
H–C(5)(y^1)	70	2.02	19.0
H–C(6)(y^2)	100	13.98	19.3
H–C(6)(y^1)	90	8.09	19.2

[a]) Observed ^{1}H-NMR signal. [b]) Extrapolated coalescence temperature. [c]) Frequency difference of the observed signals at r.t. [d]) Rotational barrier.

2.5. *Modeling of the Monomers* **10** *and* **11**. Theoretical determination of low-energy conformations and the rotational barriers of compounds **10** and **11** were performed using the semi-empirical method AM1 by *Dewar*, *Stewart*, and coworkers [19] as implemented in the program *Spartan*™ (Version 4.0). Calculations were performed in the gas phase. In a first step, an energy-minimized structure of the examined isomer was produced. Starting from this conformation, the torsion angle α was rotated gradually in 1° steps. After each 1° rotation, the angle α was fixed, and a low-energy conformation search was done. The resulting enthalpies of formation were plotted *vs.* α generating the two diagrams shown in *Figs. 7* and *9*. A set of energy-minimized structures obtained at selected torsion angles α along the structure-energy profiles for **10** and **11** are shown in *Figs. 8* and *10*.

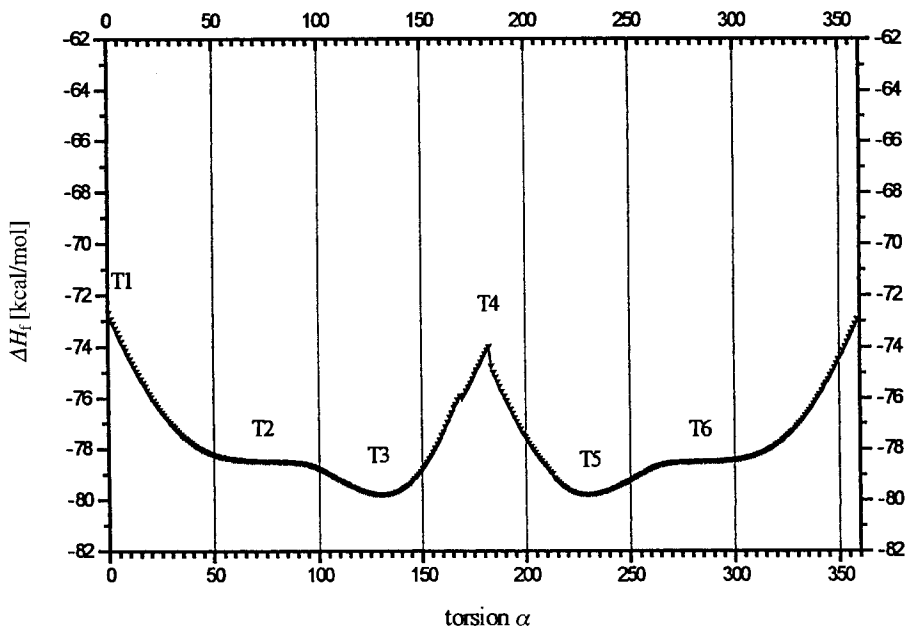

Fig. 7. *Energy profile of* **10**. The heats of formation of AM1-energy-minimized conformers are plotted *vs.* the constraint torsion angle α.

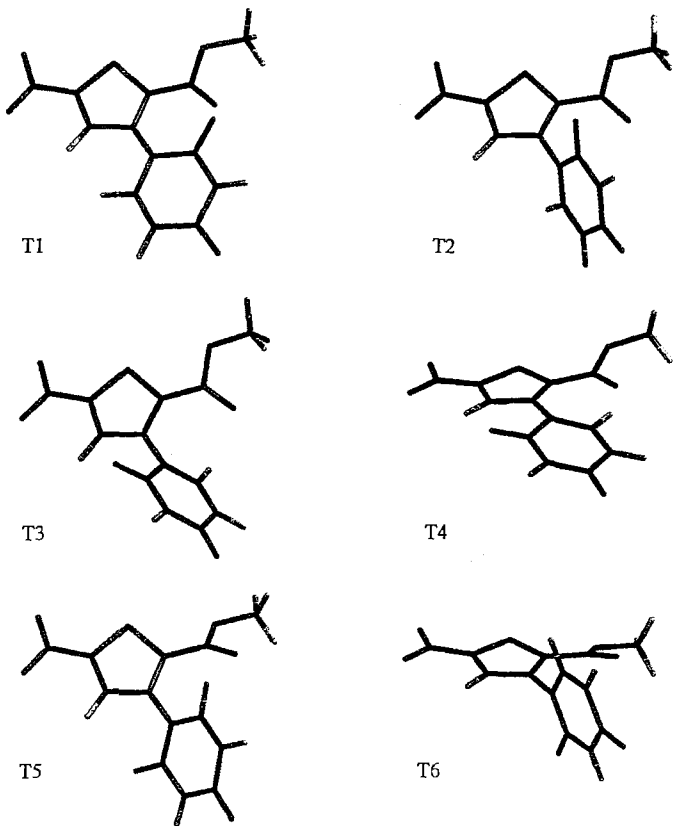

Fig. 8. *Selected conformers T1–T6 of* **10** (see *Fig. 7*)

The nitro isomer **10** shows a classic energy profile [20], with two steric barriers near 0 and 180° (conformers T1 and T4) and two weak π-barriers near 90 and 270° (conformers T2 and T6). The calculated energy difference of 7.1 kcal/mol for the energy maximum T1 (*Table 3*) stays for the rotational barrier caused by the repulsions between O(2)···O(10′) and C(6)–H···H–C(4′) (for numbering, see *Fig. 3*). The second lower rotational barrier of 5.8 kcal/mol at T4 is caused by the repulsions of C(4′)–H···O(2) and C(6)–H···O(10′). The calculated torsion-angle values of the absolute-minimum conformation T5 differs only little from the experimental X-ray data. If the observed X-ray angle values were entered, the result of a single-point calculation showed only a slightly increased enthalpy of formation of 0.71 kcal/mol relative to the absolute minimum.

The nitro isomer **11** shows again a classic energy profile [20], with two steric barriers near 0 and 180° (conformers K1 and K6) and two π-barriers near 90 and 270° (conformers K4 and K9). In between, the four local minima corresponding to the conformers K3, K5, K8, and K10 are found. The two determined energy maxima (conformers K1 and K6) differ by 0.5 kcal/mol from each other (*Table 4*). The corresponding structures are substantially distorted with a high degree of pyramidalization at the N(1)-atom of the

Table 3. *AM1-Calculated Torsion Angles α–γ and Enthalpies of the Conformers T1 to T6 for Monomer* **10**

Conformer	ΔH_f [kcal/mol]	α [°]	β [°]	γ [°]
T1	−72.647	0.095	−126.166	−7.036
T2	−78.459	68.190	−162.195	−1.476
T3	−79.774	131.366	−143.487	−1.393
T4	−73.979	182.441	− 61.646	−0.850
T5	−79.778	229.529	145.735	2.118
T6	−78.486	280.781	160.460	0.300

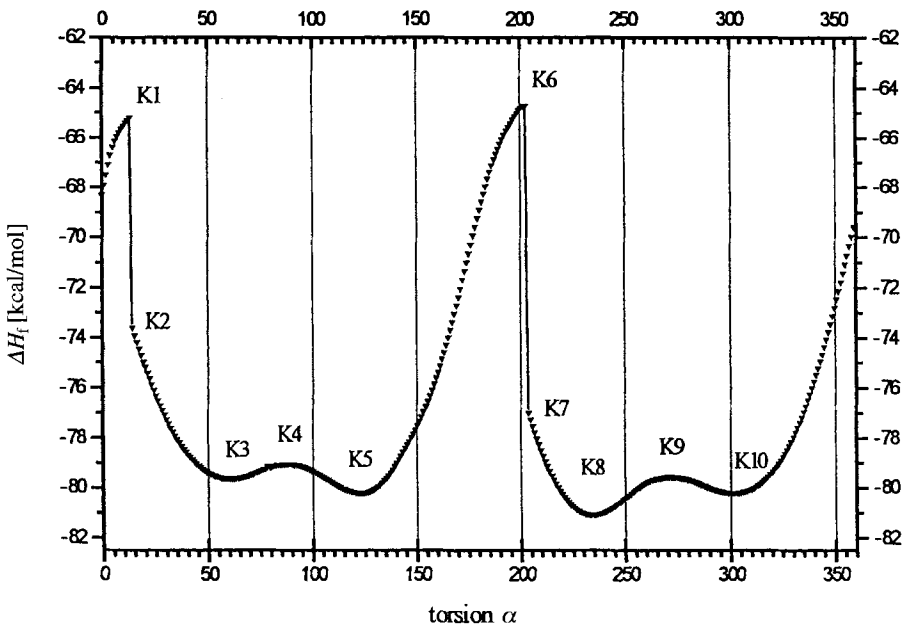

Fig. 9. *Energy profile of* **11**. The heat of formation of AM1-energy-minimized conformers are plotted *vs.* the constraint torsion angle α.

base uracil (for numbering, see *Fig. 4*). The two highest-energy conformers K1 and K6 expectedly occur at α near 0 and 180° which forces the thiophene core unit in the same plane as the uracil base. There exists a large energy gap between K1 and K2 and between K6 and K7, respectively. Structurally K1 and K2, as well K6 and K7, corresponding to only 1° rotation around α, are completely different as can be seen from *Fig. 10* and, therefore, are the consequence of a different minimization pathway. If values for α, β, and γ as determined by X-ray of **11** were entered, by a single-point energy calculation, an increased enthalpy of formation of 2.45 kcal/mol relative to the absolute minimum corresponding to K8 is obtained. This difference may be attributed either to an overestimation of the π-barrier by AM1 or to specific crystal-lattice forces or intermolecular H-bonding as observed in the crystal of **11**. The calculated rotational barrier of this compound is by 3 kcal/mol lower than the experimentally determined one in compound **16** in which the rotation around a biaryl-like axis might be influenced by intramolecular

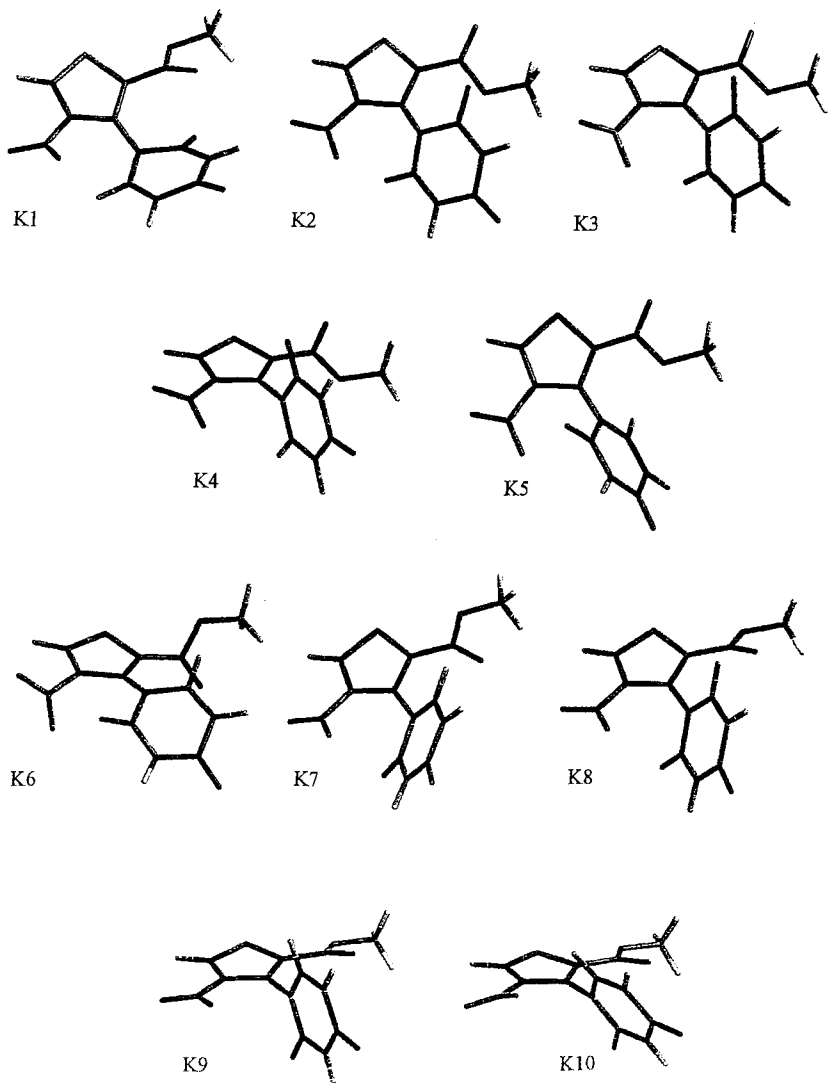

Fig. 10. *Selected conformers K1–K10 of* **11** (see *Fig. 9*)

H-bond formation between C(4')–NH and O(2). The impossibility of intramolecular H-bond formation in the model **11** can be one reason for this small energy difference between experimental and calculated value.

3. Conclusions. – We have demonstrated here that the monomer building block **13** for distamycin-NA containing the base uracil could efficiently be prepared in five steps starting from commercial available **1**. Amide-bond formation between two monomeric units was achieved by the use of the coupling reagent DCC. X-Ray analyses revealed that

Table 4. *AM1-Calculated Torsion Angles α–γ and Enthalpies of the Conformers K1 to K10 for Monomer* **11**

Conformer	ΔH_f [kcal/mol]	α [°]	β [°]	γ [°]
K1	–65.198	12.984	147.410	38.432
K2	–73.594	14.192	30.466	5.686
K3	–79.626	61.170	16.836	–23.718
K4	–79.041	87.243	23.719	–15.845
K5	–80.198	123.344	37.289	– 8.911
K6	–64.712	202.542	–112.343	–45.973
K7	–76.996	203.711	170.862	21.236
K8	–81.076	233.651	152.009	9.343
K9	–79.558	271.755	161.987	12.023
K10	–80.204	301.840	170.144	23.431

the uracil and thiophene planes are, as expected, propeller-twisted. Variable-temperature-dependent ^{1}H-NMR experiments further confirmed the isomerism in **16** caused by the biaryl-like bonds, with a transition energy of 19 ± 1 kcal/mol between two rotameric forms. These experimental results were further confirmed by AM1 calculations. If one considers that the intramolecular rotation around a biaryl-like axis is a first-order reaction, the calculated half-life is in the order of 10 to 3 s for the temperature range 25–37°. Fast interconversion of rotamers at room temperature and at slightly elevated temperatures is, therefore, possible. From this, it can be concluded that DNA recognition should not be hindered by a restricted rotation around the biaryl-like axis in distamycin-NA. These initial results encouraged us to synthesize oligomers thereof and to investigate the pairing properties of distamycin-NA containing the base uracil, with single- and double-stranded RNA and DNA, respectively. These results will be reported soon.

We gratefully acknowledge financial support from the *Swiss National Science Foundation* (grant No. 2000-49'191.96) and from the *Wander-Stiftung*. We thank Prof. Dr. *H. B. Bürgi* and *S. Capelli* for the opportunity and technical assistance in X-ray structure determination. We also thank Dr. *C. Müller* for the temperature-dependent ^{1}H- and ^{13}C-NMR experiments and Dr. *J. Hunziker* for the help in AM1 calculation.

Experimental Part

General. DCC = *N,N'*-dicyclohexylcarbodiimide, BtOH = 1-hydroxy-1*H*-benzotriazole hydrate. Solvents for reactions: Et_2O, distilled over $LiAlH_4$; THF, distilled over Na; AcOH, freshly crystallized; EtOH, *puriss. p.a.*, MeOH, *puriss. p.a.*; DMF, *puriss. p.a.*; benzene, *puriss. p.a.*, was used as purchased from *Fluka*; dioxane was filtered over basic alox before use. Solvent for chromatography and workup: technical grade, distilled over *Sikkon* (anh. $CaSO_4$, *Fluka*). Chemicals for reactions: from *Fluka*, except 100% HNO_3 (*Merck*), BtOH (*Aldrich*), and 10% Pd/C (*Heraeus*). TLC: silica gel *G-25 UV$_{254}$* precoated glass plates, *Macherey-Nagel*; detection either by UV or by spraying a soln. of 0.3 g ninhydrin in BuOH (100 ml) and AcOH (3 ml) followed by heating with a heat gun. Flash chromatography (FC): silica gel 30–60 μm, *J. T. Baker*. M.p.: *Büchi-510* melting-point apparatus, open capillaries; uncorrected. UV/VIS Spectra: *Varian-Cary-3E* spectrophotometer; λ_{max} in nm (ε). IR Spectra: *Perkin-Elmer-1600-FTIR* spectrometer; $\tilde{\nu}$ in cm^{-1}. NMR Spectra: *Bruker-AC-300* spectrometer, at 300 (^{1}H) and 75 MHz (^{13}C) in (D_6)DMSO; δ in ppm *vs.* solvent as internal ref. (δ(H) 2.49, δ(C) 39.70); ^{13}C multiplicities from DEPT spectra. MS: *Varian-MAT-CH-7A*; EI, ionization energy 70 eV; *AutoSpec Q VG*, FAB (positive), matrix solvent (dithiothreitol); *m/z* (rel. %). Elemental analyses: Microanalytical Laboratory of the Laboratorium für Organische Chemie, ETH-Zürich.

Methyl 3-(Acetylamino)-5-nitro- and 4-nitrothiophene-2-carboxylate (**2** and **3**, resp.). To a cooled (–35°) and mechanically stirred soln. of methyl 3-(acetylamino)thiophene-2-carboxylate (**1**; 15 g, 75.3 mmol) in 95%

H_2SO_4 (150 ml), 100% HNO_3 (15 ml) was added. The mixture was stirred at $-25°$ for 45 min and allowed to warm up to 0°. The viscous liquid was poured on ice (250 g) the resulting aq. phase extracted with CH_2Cl_2 (5 × 300 ml), the org. layer dried ($MgSO_4$) and evaporated, and the crude dissolved in hot toluene to saturation at 100°. Product **3** (6.4 g, 35%) crystallized overnight at 4° as faint yellow needles and was filtered off. Concentration of the filtrate to 1/2 volume followed by standing at 4° for another night yielded a second crop of **3** that was contaminated with *ca.* 5–10% of **2**. The resulting filtrate was evaporated and dried *in vacuo*: **2** (9.35 g, 51%). Dark yellow powder.

Data of **3**: TLC (Et_2O/hexane 6:4): R_f 0.18. M.p. 172–174°. UV/VIS (MeCN): 200 (11500), 254 (16000). IR (KBr): 3420*w*, 3268*m*, 3126*m*, 3098*m*, 3014*w*, 2958*w*, 1720*s*, 1694*s*, 1666*s*, 1570*s*, 1534*s*, 1501*s*, 1441*m*, 1415*m*, 1355*s*, 1270*s*, 1191*s*, 1107*s*, 1076*w*, 1037*w*, 1007*m*, 994*m*, 950*w*, 900*m*, 854*w*, 826*w*, 812*w*, 806*w*, 776*m*, 759*m*, 732*m*, 716*m*, 679*w*, 634*w*, 569*m*, 538*w*, 484*w*. ^{1}H-NMR: 2.07 (*s*, MeCON–C(3)); 3.83 (*s*, MeOCO–C(2)); 8.87 (*s*, H–C(5)); 10.24 (*s*, NH–C(3)). ^{13}C-NMR: 23.19 (*q*); 53.30 (*q*); 122.01 (*s*); 133.39 (*d*); 143.35 (*s*); 161.15 (*s*); 169.60 (*s*). EI-MS: 244 (4, M^+), 202 (100), 170 (36), 156 (5), 97 (8), 96 (7), 69 (7), 59 (5), 52 (14), 45 (9), 43 (53), 28 (12).

Data of **2**: TLC (Et_2O/hexane 6:4): R_f 0.33. M.p. 115–116°. UV/VIS (MeCN): 220 (sh, 7100), 257 (16800), 295 (9700), 372 (4400). IR (KBr): 3450*w*, 3329*m*, 3154*w*, 2965*w*, 1708*s*, 1694*s*, 1579*s*, 1528*s*, 1488*w*, 1449*m*, 1434*s*, 1370*w*, 1341*s*, 1271*s*, 1237*m*, 1210*m*, 1099*w*, 1057*w*, 1040*w*, 1000*w*, 952*w*, 859*w*, 818*w*, 768*m*, 730*w*, 668*w*, 655*w*, 588*w*, 556*w*. ^{1}H-NMR: 2.18 (*s*, MeCON–C(3)); 3.88 (*s*, MeOCO–C(2)); 8.57 (*s*, H–C(4)); 10.01 (*s*, NH–C(3)). ^{13}C-NMR: 23.94 (*q*); 53.25 (*q*); 116.04 (*s*); 123.26 (*d*); 140.66 (*s*); 152.56 (*s*); 162.02 (*s*); 168.72 (*s*). EI-MS: 244 (16, M^+), 202 (59), 199 (43), 187 (13), 170 (30), 157 (100), 156 (25), 152 (6), 126 (31), 125 (93), 110 (7), 97 (14), 82 (9), 69 (10), 59 (14), 45 (13), 43 (66).

Methyl 3-Amino-4-nitrothiophene-2-carboxylate (**5**). To a suspension of **3** (10 g, 41.0 mmol) in MeOH (600 ml) was added dropwise a soln. of NaOMe in MeOH prepared *in situ* from Na (1.2 g, 52.2 mmol) in MeOH (83 ml) and heated to 55–60° for 1 h (TLC monitoring). The mixture was cooled to 0–5°, then H_2O (200 ml) was added. The resulting yellow precipitate was filtered, washed with H_2O (20 ml), and dried *in vacuo*: **5** (6.7 g, 80%). TLC (Et_2O/hexane 6:4): R_f 0.67. M.p. 119°. UV/VIS (MeCN): 196 (8300), 238 (13400), 276 (14900), 391 (3200). IR (KBr): 3487*m*, 3462*m*, 3382*w*, 3351*s*, 3108*m*, 3086*m*, 2955*w*, 1683*s*, 1607*s*, 1548*m*, 1486*s*, 1451*s*, 1428*m*, 1346*m*, 1303*s*, 1218*s*, 1185*w*, 1140*w*, 1116*m*, 1072*w*, 974*w*, 910*w*, 857*w*, 832*w*, 808*w*, 790*w*, 770*s*, 740*m*, 668*m*. ^{1}H-NMR: 3.77 (*s*, MeOCO–C(2)); 7.12 (*s*, NH_2–C(3)); 8.92 (*s*, H–C(5)). ^{13}C-NMR: 51.78 (*q*); 99.97 (*s*); 136.42 (*d*); 147.09 (*s*); 163.16 (*s*). EI-MS: 204 (9), 203 (13), 202 (100, M^+), 172 (5), 171 (35), 170 (48), 154 (6), 125 (6), 97 (11), 96 (8), 69 (7), 52 (9), 45 (7), 32 (18), 28 (41).

Methyl-3-Amino-5-nitrothiophene-2-carboxylate (**4**). As described for **5**, with **2** (6 g, 24.6 mmol), MeOH (360 ml), Na (0.6 g, 26.1 mmol) in MeOH (60 ml); 1/2 h and H_2O (120 ml). The resulting dark red precipitate was taken up in CH_2Cl_2 (150 ml), the insoluble blue polymer filtered off, and the filtrate slowly evaporated: **4** (3.1 g, 62%). Red needles. TLC (Et_2O/hexane 6:4): R_f 0.42. M.p. 167–169°. UV/VIS (MeCN): 221 (6500), 258 (10500), 300 (9000), 426 (3900). IR (KBr): 3468*m*, 3362*m*, 3096*w*, 2957*w*, 1693*s*, 1662*w*, 1619*s*, 1572*w*, 1553*m*, 1509*m*, 1450*m*, 1427*w*, 1344*s*, 1277*s*, 1232*m*, 1193*w*, 1129*m*, 1095*m*, 1070*w*, 948*w*, 925*w*, 856*w*, 817*w*, 789*w*, 768*m*, 729*w*, 668*w*, 648*w*, 606*w*. ^{1}H-NMR: 3.77 (*s*, MeOCO–C(2)); 6.82 (*s*, NH_2–C(3)); 7.47 (*s*, H–C(4)). ^{13}C-NMR: 52.05 (*q*); 101.96 (*s*); 120.98 (*d*); 152.10 (*s*); 152.37 (*s*); 163.44 (*s*). EI-MS: 202 (100, M^+), 172 (11), 171 (35), 170 (87), 156 (9), 144 (8), 125 (12), 113 (9), 97 (18), 96 (23), 86 (33), 84 (55), 71 (6), 70 (13), 69 (20), 68 (17), 59 (7), 52 (13), 45 (11), 32 (9).

Methyl 3-{{[(3-Methoxy-1-oxoprop-2-enyl)amino]carbonyl}amino}-4-nitrothiophene-2-carboxylate (**7**). To a soln. of 3-methoxyacryloyl chloride (6.5 g, 54.0 mmol) [21] in benzene (108 ml), AgOCN (16.2 g, 108.0 mmol) was added and the mixture refluxed for 30 min. After sedimentation of the inorg. salts, the liquid layer was added dropwise to a cooled (−20°) soln. of **5** (5.4 g, 26.71 mmol) in DMF (310 ml) and Et_2O (103 ml). After addition was completed, the mixture was stirred 1.5 h at −10°, then allowed to warm up to r.t., stirred for 3.5 h, and quenched with AcOEt (1400 ml). The org. layer was extracted with H_2O (4 × 200 ml) and evaporated. The resulting yellow-white crude material was washed with a minimum of *t*-BuOMe to furnish **7** (6.70 g, 76%) as a white powder that was contaminated with 3-methoxyacrylic acid (4%; by ^{1}H-NMR). For the anal. data, the mixture (100 mg) was dissolved in dioxane/H_2O 4:1 (50 ml), adsorbed on silica gel (1 g), and purified by FC (MeOH/CH_2Cl_2 0.2:10). TLC (MeOH/CH_2Cl_2 0.5:12): R_f 0.55. M.p. 193–195°. UV/VIS (MeCN): 252 (53500). IR (KBr): 3436*w*, 3235*w*, 3109*w*, 1712*m*, 1686*m*, 1610*m*, 1569*m*, 1534*w*, 1504*m*, 1447*w*, 1363*w*, 1341*w*, 1284*m*, 1257*w*, 1231*w*, 1212*w*, 1187*w*, 1148*m*, 1115*w*, 1087*w*, 1006*w*, 988*w*, 842*w*, 821*w*, 778*w*, 755*w*, 729*w*, 668*w*, 608*w*, 538*w*. ^{1}H-NMR: 3.73 (*s*, 3 H); 3.84 (*s*, 3 H); 5.57 (*d*, J = 12.1, 1 H); 7.74 (*d*, J = 12.1, 1 H); 8.86 (*s*, H–C(5)); 10.73 (*s*, NH); 11.62 (*s*, NH). ^{13}C-NMR: 53.12 (*q*); 58.77 (*q*); 97.72 (*d*); 119.14 (*s*); 132.80 (*s*); 133.07 (*d*); 142.60 (*s*); 151.20 (*s*); 161.33 (*s*); 164.66 (*d*); 168.09 (*s*). EI-MS: 329 (1, M^+), 297 (5), 251 (11), 228 (7), 203 (7), 202 (88),

197 (11), 171 (26), 170 (35), 156 (8), 127 (8), 97 (19), 96 (16), 86 (8), 85 (100), 70 (15), 69 (15), 53 (14), 52 (24), 45 (16).

Methyl 3-{{[(3-Methoxy-1-oxoprop-2-enyl)amino]carbonyl}amino}-5-nitrothiophene-2-carboxylate **6**. As described for 7, with 3-methoxyacryloyl chloride (2.41 g, 20.0 mmol), benzene (40 ml), AgOCN (6 g, 40 mmol), and **4** (2 g, 9.9 mmol) in DMF (115 ml) and Et_2O (38 ml) at $-30°$, then 2.5 h at $-10°$ and standing overnight at 4°. The bright yellow precipitate **6** was filtered off the filtrate evaporated, and the resulting orange-yellow residue washed with *t*-BuOMe (20 ml) and CH_2Cl_2 (20 ml), yielding a total of 3.2 g (98%) of **6**. TLC ($MeOH/CH_2Cl_2$ 0.5:12): R_f 0.61. M.p. 255°. UV/VIS (MeCN): 240 (sh, 17800), 266 (31000), 297 (sh, 11500), 374 (4100). IR (KBr): 3428*w*, 3237*m*, 3143*m*, 2866*w*, 2850*w*, 1712*s*, 1689*s*, 1621*s*, 1576*s*, 1526*s*, 1446*m*, 1417*w*, 1341*s*, 1310*w*, 1268*s*, 1229*m*, 1212*m*, 1190*w*, 1146*s*, 1094*m*, 1040*w*, 990*w*, 973*w*, 934*w*, 862*w*, 816*m*, 770*m*, 752*w*, 728*w*, 668*w*, 640*w*, 602*w*, 566*w*, 524*w*, 475*w*. ^{1}H-NMR: 3.73 (*s*, 3 H); 3.90 (*s*, 3 H); 5.58 (*d*, J = 12.1, 1 H); 7.74 (*d*, J = 12.5, 1 H); 8.71 (*s*, H–C(4)); 10.78 (*s*, NH); 12.37 (*s*, NH). EI-MS: 329 (8, M^+), 297 (7), 202 (37), 170 (27), 85 (100), 73 (12.21), 59 (14).

4-Nitro-3-(1',2',3',4'-tetrahydro-2',4'-dioxopyrimidin-1'-yl)thiophene-2-carboxylic Acid (**9**) *and Methyl 4-Nitro-3-(1,2,3,4-tetrahydro-2,4-dioxopyrimidin-1-yl)thiophene-2-carboxylate* (**11**). A suspension of finely ground **7** (1.4 g, 4.25 mmol) in 2M H_2SO_4 (235 ml) was refluxed for 1.75 h. The mixture was then cooled to 0°. After 2 h, the yellow precipitate (1.04 g) was filtered off and air-dried. The solid material was dissolved in dioxane/H_2O 4:1 (150 ml) and adsorbed on silica gel (7 g). FC ($MeOH/CH_2Cl_2$ 0.25:10) furnished **11** (0.618 g, 49%) as a white powder. Further elution with EtOH gave **9** (0.313 g, 26%) as a faint yellow powder.

Data of **11**: TLC ($MeOH/CH_2Cl_2$ 0.5:12): R_f 0.45. M.p. 239–240°. UV/VIS (MeCN): 203 (14700), 241 (21400), 254 (sh, 19800). IR (KBr): 3433*m*, 3109*m*, 3048*m*, 2921*w*, 2841*w*, 1726*s*, 1694*s*, 1628*m*, 1560*s*, 1518*s*, 1439*s*, 1427*m*, 1384*m*, 1344*m*, 1293*s*, 1276*s*, 1210*m*, 1106*m*, 974*w*, 950*w*, 890*w*, 846*w*, 836*w*, 813*w*, 799*w*, 767*w*, 719*w*, 692*w*, 648*w*, 561*w*, 436*w*. ^{1}H-NMR: 3.83 (*s*, MeOCO–C(2)); 5.79 (*d*, J = 7.7, H–C(5')); 7.72 (*d*, J = 7.7, H–C(6')); 9.17 (*s*, H–C(5)); 11.70 (*s*, H–N(3')). ^{13}C-NMR: 53.35 (*d*); 101.94 (*d*, C(5')); 129.79 (*s*); 132.53 (*s*); 134.91 (*d*, C(5)); 142.60 (*s*); 145.05 (*d*, C(6')); 150.03 (*s*); 159.22 (*s*); 163.70 (*s*). EI-MS: 297 (54, M^+), 266 (8), 251 (100), 239 (12), 197 (7), 195 (14), 194 (6), 192 (10), 168 (10), 156 (30), 121 (5), 109 (8), 96 (16), 95 (6), 94 (10), 81 (13), 70 (19), 69 (32), 59 (19). Anal. calc. for $C_{10}H_7N_3O_6S$ (297.25): C 40.41, H 2.37, N 14.14, O 32.30, S 10.79; found: C 40.20, H 2.32, N 14.16, O 32.06, S 11.06.

Data of **9**: TLC ($MeOH/CHCl_3$/AcOH 4:6:0.5): R_f 0.52. M.p. 227–228°. UV/VIS (H_2O): 210 (16300), 241 (16100), 258 (16100). IR (KBr): 3437*m*, 3126*m*, 1692*s*, 1622*m*, 1561*m*, 1516*m*, 1436*m*, 1345*m*, 1292*m*, 1225*w*, 1115*w*, 1090*w*, 900*w*, 874*w*, 818*w*, 772*w*, 721*w*, 679*w*, 668*w*, 648*w*, 567*w*, 432*w*. ^{1}H-NMR: 5.69 (*dd*, J = 7.7, 2.2, H–C(5')); 7.64 (*d*, J = 7.7, H–C(6')); 8.96 (*s*, H–C(5)); 11.54 (*d*, J = 1.8, H–N(3')). ^{13}C-NMR: 101.33 (*d*, C(5')); 129.69 (*s*); 132.64 (*d*, C(5)); 137.31 (*s*); 142.49 (*s*); 146.26 (*d*, C(6')); 150.31 (*s*); 160.80 (*s*); 164.11 (*s*). EI-MS: 283 (1, M^+), 251 (11), 239 (9), 196 (12), 193 (15), 111 (5), 98 (6), 83 (6), 82 (7), 81 (5), 70 (7), 69 (17), 68 (7), 67 (5), 58 (9), 52 (7), 44 (100).

X-Ray Structure of **11**. Transparent colorless prism (0.35 × 0.21 × 0.21 mm); $C_{10}H_7N_3O_6S$; monoclinic space group $P2_1/n$, Z = 4; a = 11.837(1), b = 8.996(1), c = 12.065(1) Å. Intensities were measured with a *Siemens SMART CCD* diffractometer (MoK_α, λ = 0.71073 Å). Of the 1727 independent reflections ($\theta < 23.3°$), 1636 with $F > 4\sigma(F)$ were used in the refinement. The structure was solved using direct methods with SHELXS-86 [22] and refined by full-matrix least-squares procedures SHELXL-93 [23]. Non-H-atoms were refined anisotropically. The positions of the H-atoms were calculated and included in the final structure-factor calculation. The refinement converged at R = 0.0318, R_w = 0.0824.

5-Nitro-3-(1',2',3',4'-tetrahydro-2',4'-dioxopyrimidin-1'-yl)thiophene-2-carboxylic Acid (**8**). A suspension of ground **6** (1.4 g, 4.25 mmol) in 2M H_2SO_4 (235 ml) was refluxed for 12.75 h. The mixture was then cooled to r.t. and allowed to stand at 4° overnight. The resulting grey precipitate was filtered off and dried *in vacuo*: **8** (1.0 g, 83%). TLC ($MeOH/CHCl_3$/AcOH 4:6:0.5): R_f 0.54. M.p. 260–262° (dec.). UV/VIS (H_2O): 200 (sh, 13200), 220 (sh, 10700), 264 (14100), 297 (sh, 10000). IR (KBr): 3440*w*, 3245*m*, 3111*m*, 2855*w*, 2580*w*, 1727*s*, 1691*s*, 1663*s*, 1550*w*, 1526*s*, 1456*m*, 1428*m*, 1376*w*, 1342*m*, 1293*m*, 1261*m*, 1227*m*, 1084*w*, 968*w*, 870*w*, 818*w*, 754*w*, 732*w*, 682*w*, 610*w*, 558*w*, 478*w*. ^{1}H-NMR: 5.71 (*dd*, J = 7.9, 2.0, H–C(5')); 7.71 (*d*, J = 8.1, H–C(6')); 8.37 (*s*, H–C(4)); 11.61 (*d*, J = 1.5, H–N(3')). ^{13}C-NMR: 101.62 (*d*, C(5')); 130.45 (*d*, C(4)); 134.83 (*s*); 137.33 (*s*); 145.29 (*d*, C(6')); 150.14 (*s*); 150.63 (*s*); 160.38 (*s*); 163.84 (*s*). EI-MS: 283 (5, M^+), 240 (26), 239 (42), 196 (83), 193 (22), 170 (8), 168 (12), 155 (7), 138 (19), 124 (9), 122 (44), 96 (9), 95 (13), 82 (9), 69 (16), 62 (12), 52 (5), 45 (35), 44 (100), 43 (7). Anal. calc. for $C_9H_5N_3O_6S$ (283.22): C 38.17, H 1.78, N 14.84, O 33.89, S 11.32; found: C 38.27, H 1.80, N 14.81, O 34.19, S 11.53.

Methyl 5-Nitro-3-(1',2',3',4'-tetrahydro-2',4'-dioxopyrimidin-1'-yl)thiophene-2-carboxylate (**10**). To a suspension of **8** (1.0 g, 3.5 mmol) in MeOH (140 ml), a soln. of $BF_3 \cdot Et_2O$ (40 ml) was added. After 72 h of reflux, the

mixture was neutralized with sat. $NaHCO_3$ soln. (250 ml) under ice-cooling and extracted with CH_2Cl_2 (4 × 120 ml), the combined org. phase dried ($MgSO_4$) and evaporated, and the resulting yellow residue washed with CH_2Cl_2 in small portions and then dried *in vacuo*: **10** (0.73 g, 70%). Faint yellow powder. TLC (MeOH/CH_2Cl_2 0.5:12): R_f 0.45. M.p. 247–249°. UV/VIS (MeCN): 260 (17100), 288 (sh, 14100). IR (KBr): 3434*m*, 3134*m*, 3103*m*, 3042*m*, 2853*w*, 1733*s*, 1702*s*, 1624*w*, 1558*w*, 1529*s*, 1456*w*, 1434*m*, 1404*m*, 1378*w*, 1346*s*, 1286*s*, 1224*m*, 1122*w*, 1110*w*, 1086*w*, 991*w*, 948*w*, 869*w*, 820*m*, 766*w*, 753*w*, 727*w*, 669*w*, 596*w*, 563*w*, 545*w*, 481*w*. ^{1}H-NMR: 384 (*s*, MeOCO–C(2)); 5.74 (*d*, *J* = 7.7, H–C(5′)); 7.72 (*d*, *J* = 7.7, H–C(6′)); 8.41 (*s*, H–C(4)); 11.65 (*s*, H–N(3′)). ^{13}C-NMR: 53.57 (*d*); 101.80 (*d*, C(5′)); 130.23 (*d*, C(4)); 131.78 (*s*); 137.96 (*s*); 144.97 (*d*, C(6′)); 150.00 (*s*); 151.17 (*s*); 159.24 (*s*); 163.68 (*s*). EI-MS: 297 (58, M^+), 267 (6), 255 (6), 254 (59), 240 (10), 239 (100), 226 (10), 196 (38), 168 (8), 109 (7), 69 (22). Anal. calc. for $C_{10}H_7N_3O_6S$ (297.25): C 40.41, H 2.37, N 14.14, O 32.30, S 10.79; found: C 40.34, H 2.35, N 14.07, O 32.23, S 11.01.

X-Ray Structure of **10**. Transparent yellow prism (0.48 × 0.35 × 0.35 mm); $C_{10}H_7N_3O_6S$; monoclinic space group $P2_1/c$, $Z = 4$; $a = 3.905(1)$, $b = 16.141(5)$, $c = 19.286(6)$ Å. Intensities were measured with an *Enraf-Nonius-CAD-4* diffractometer (MoK_α, $\lambda = 0.71069$ Å). Of the 2746 independent reflections ($\theta < 27.5°$), 2328 with $F > 4\sigma(F)$ were used in the refinement. The further procedure was as described for **11**. The refinement converged at $R = 0.0343$, $R_w = 0.1014$.

Methyl 4-Amino-3-(1′,2′,3′,4′-tetrahydro-2′,4′-dioxopyrimidin-1′-yl)thiophene-2-carboxylate (**13**) *and Methyl 4-(Acetylamino)-3-(1′,2′,3′,4′-tetrahydro-2′,4′-dioxopyrimidin-1′-yl)thiophene-2-carboxylate* (**14**). To a suspension of **11** (1.0 g, 3.36 mmol) in degassed THF/AcOH 5:1 (240 ml), 10% Pd/C (1.0 g) was added, and the resulting mixture was hydrogenated with H_2 at normal pressure. After 55 min, the mixture was filtered through a silica gel (40 g) slurry in MeOH. The silica gel was washed with MeOH (250 ml), and dioxane/H_2O 4:1 (30 ml) was added to the filtrate, which was concentrated to ½ volume. Then further dioxane/H_2O 4:1 (50 ml) and toluene (30 ml) were added followed by concentrating to ⅕ volume. Finally, dioxane/H_2O 4:1 (50 ml) and toluene (150 ml) were added followed by complete evaporation. The yellow residue (2.0 g) was dissolved in dioxane/H_2O 4:1 (70 ml) and adsorbed on silica gel (14 g). Purification by FC silica gel (90 g), EtOH/CH_2Cl_2 (0.5:10) yielded **13** (0.690 g, 77%) and **14** (31 mg, 3%) as white powders.

Data of **13**: TLC (EtOH/CH_2Cl_2 0.8:10): R_f 0.16. M.p. 195–196°. UV/VIS (MeCN): 200 (19900), 254 (12500), 331 (4300). IR (KBr): 3413*m*, 3093*w*, 2955*w*, 2853*w*, 1701*s*, 1631*m*, 1560*w*, 1489*m*, 1439*m*, 1416*m*, 1383*m*, 1306*m*, 1280*m*, 1236*m*, 1090*m*, 1020*w*, 960*w*, 876*w*, 817*w*, 769*m*, 668*w*, 627*w*, 598*w*, 552*w*, 502*w*. ^{1}H-NMR: 3.70 (*s*, MeOCO–C(2)); 5.17 (*s*, H_2N–C(4)); 5.62 (*d*, *J* = 8.1, H–C(5′)); 6.53 (*s*, H–C(5)); 7.37 (*d*, *J* = 7.7, H–C(6′)); 11.35 (*s*, H–N(3′)). ^{13}C-NMR: 52.20 (*q*, *Me*OCO–C(2)); 101.97 (*d*, C(5′)); 103.63 (*d*, C(5)); 124.84 (*s*); 130.77 (*s*); 145.10 (*s*); 145.61 (*d*, C(6′)); 150.17 (*s*); 160.56 (*s*); 164.30 (*s*). EI-MS: 269 (11), 268 (14), 267 (100, M^+), 224 (5), 193 (5), 192 (36), 165 (6), 164 (15), 151 (8). Anal. calc. for $C_{10}H_9N_3O_4S$ (267.26): C 40.94, H 3.39, N 15.72, O 23.95, S 12.00; found: C 40.93, H 3.54, N 15.49, O 24.13, S 11.90.

Data of **14**: TLC (EtOH/CH_2Cl_2 0.8:10): R_f 0.12. M.p. 265–266° (dec.). UV/VIS (MeCN): 202 (24900), 228 (28100), 301 (sh, 7600). IR (KBr): 3435*m*, 3330*m*, 3220*m*, 3054*w*, 2947*w*, 2870*w*, 1702*s*, 1683*s*, 1638*m*, 1572*m*, 1545*m*, 1475*m*, 1446*m*, 1397*m*, 1299*m*, 1278*s*, 1207*m*, 1111*m*, 1038*m*, 812*w*, 779*w*, 668*w*, 632*w*, 594*w*, 559*w*, 518*w*. ^{1}H-NMR: 2.04 (*s*, MeCONH–C(4)); 3.74 (*s*, MeOCO–C(2)); 5.66 (*d*, *J* = 7.7, H–C(5′)); 7.45 (*d*, *J* = 7.7, H–C(6′)); 8.18 (*s*, H–C(5)); 9.92 (*s*, NH–C(4)); 11.42 (*s*, H–N(3′)). ^{13}C-NMR: 23.61 (*q*, MeCONH–C(4)); 52.95 (*q*, *Me*OCO–C(2)); 102.62 (*d*, C(5′)); 117.19 (*d*, C(5)); 125.69 (*s*); 132.44 (*s*); 134.58 (*s*); 145.86 (*d*, C(6′)); 150.72 (*s*); 160.59 (*s*); 164.90 (*s*); 169.40 (*s*). EI-MS: 309 (51, M^+), 269 (7), 268 (14), 267 (100), 224 (12), 193 (9), 192 (59), 191 (8), 166 (8), 164 (23), 151 (14), 137 (6), 136 (6), 57 (6), 43 (39).

Methyl 5-Amino-3-(1′,2′,3′,4′-tetrahydro-2′,4′-dioxopyrimidin-1′-yl)thiophene-2-carboxylate (**12**). To a soln. of **10** (0.50 g, 1.68 mmol) in degassed THF/AcOH 5:1 (120 ml), 10% Pd/C (0.50 g) was added, and the resulting mixture was hydrogenated with H_2 at normal pressure. After 18 h, the mixture was filtered over *Celite*, the latter washed with MeOH (200 ml) and toluene (100 ml), and the filtrate concentrated to *ca.* ⅕ volume. Then further toluene (300 ml) was added followed by evaporation to dryness. To remove traces of residual AcOH, the residue was dissolved in dioxane/H_2O 4:1 and the soln. co-evaporated with toluene and EtOH. This was repeated 3 times. The resulting crude material (580 mg) contained 3% of AcOH (^{1}H-NMR). For the anal. data, this material (100 mg) was dissolved in dioxane/H_2O 4:1, adsorbed on silica gel (1 g), and purified by FC (MeCN/CH_2Cl_2/Et_3N 5:5:0.05): pure **12** (62 mg). Yellow powder. TLC (MeOH/CH_2Cl_2/Et_3N 1:10:0.05): R_f 0.34. M.p. 254–256° (dec.). UV/VIS (MeCN): 237 (12000), 298 (14200). IR (KBr): 3428*m*, 3326*m*, 3194*m*, 3083*w*, 2954*w*, 2853*w*, 1696*s*, 1624*m*, 1550*m*, 1476*m*, 1439*m*, 1382*w*, 1286*m*, 1190*w*, 1120*m*, 1088*m*, 808*w*, 758*w*, 690*w*, 604*w*, 582*w*, 555*w*. ^{1}H-NMR: 3.62 (*s*, MeOCO–C(2)); 5.58 (*d*, *J* = 8.1, H–C(5′)); 5.95 (*s*, H–C(4)); 7.02 (*s*, NH_2–C(5)); 7.50 (*d*, *J* = 8.1, H–C(6′)); 11.36 (*s*, H–N(3′)). ^{13}C-NMR: 51.42 (*q*, *Me*OCO–C(2)); 100.93 (*d*, C(5′)); 104.58 (*d*, C(4)); 142.01 (*s*); 145.75 (*d*, C(6′)); 149.89 (*s*); 159.84 (*s*); 160.61 (*s*); 163.97 (*s*). EI-MS: 267 (20, M^+), 224 (7),

219 (6), 181 (10), 169 (22), 131 (18), 126 (9), 119 (21), 87 (14), 86 (15), 84 (29), 76 (7), 69 (49), 66 (28), 58 (6), 43 (26), 32 (11), 28 (34), 18 (100), 17 (20).

Methyl 4-{{[4-Nitro-3-(1',2',3',4'-tetrahydro-2',4'-dioxopyrimidin-1'-yl)-2-thienyl]carbonyl}amino}-3-(1,2,3,4-tetrahydro-2,4-dioxopyrimidin-1-yl)thiophene-2-carboxylate (**16**). To a soln. of **13** (142 mg, 0.53 mmol), **9** (150 mg, 0.53 mmol), and BtOH (81 mg, 0.53 mmol) in DMF (1 ml), DCC (262 mg, 1.27 mmol) in DMF (0.5 ml) was added. The mixture was stirred under Ar for 24 h and quenched with dioxane/H_2O 4:1 (4 ml). The resulting white precipitate was filtered off and washed with additional dioxane/H_2O 4:1 (10 ml) and the filtrate evaporated. The green waxy residue was dissolved in dioxane/H_2O 4:1 (40 ml) and EtOH (10 ml) and adsorbed on silica gel (7.5 g). Purification by FC (CH_2Cl_2/EtOH/25% NH_3 soln. 10:0.5:0.05 → 10:4:0.05) yielded **16** (166 mg, 59%). Faint yellow powder. TLC (CH_2Cl_2/MeOH/25% NH_3 soln. 9:1:0.05): R_f 0.34. UV/VIS (100 mM NaCl, 10 mM Na_2HPO_4, pH 7.0): 203 (21500), 254 (23700). IR (KBr): 3440*s*, 3210*m*, 3087*m*, 3058*m*, 2961*w*, 2925*w*, 2855*w*, 1717*s*, 1690*s*, 1665*s*, 1565*m*, 1530*m*, 1436*m*, 1397*m*, 1382*m*, 1348*m*, 1311*m*, 1286*m*, 1207*w*, 1167*w*, 1097*m*, 1020*m*, 956*w*, 890*w*, 872*w*, 810*m*, 786*w*, 718*w*, 702*w*, 667*w*, 627*w*, 559*w*. ^{1}H-NMR (for numbering, see *Fig. 5*; two rotamers): 3.76 (*s*, MeOOC–C(2')(y^2)); 5.65, 5.68 (2*dd*, J = 7.7, 2.2, J = 7.7, 2.2, H–C(5)(y^2)); 5.747, 5.754 (2*d*, J = 7.7, J = 8.1, H–C(5)(y^1)); 7.49, 7.54 (2*d*, each J = 8.1, H–C(6)(y^2)); 7.65, 7.68 (2*d*, each J = 7.4, H–C(6)(y^2)); 8.212, 8.217 (2*s*, H–C(5')(y^2)); 9.05 (*s*, H–C(5')(y^1)); 10.85 (*s*, NH–C(4')(y^2)); 11.42, 11.44 (2*d*, J = 1.8, J = 2.2 H–N(3)(y^2)); 11.61, 11.63 (2*d*, each J = 1.8, H–N(3)(y^1)). ^{13}C-NMR (two rotamers): 52.72 (*q*); 101.92 (*d*); 102.03 (*d*); 102.13 (*d*); 120.64 (*d*); 120.74 (*d*); 125.89 (*s*); 126.07 (*s*); 130.02 (*s*); 130.17 (*s*); 132.07 (*d*); 132.23 (*d*); 133.05 (*s*); 133.46 (*s*); 133.55 (*s*); 134.02 (*s*); 141.95 (*s*); 142.10 (*s*); 145.16 (*d*); 145.29 (*d*); 145.53 (*d*); 145.29 (*d*); 150.19 (*s*); 150.33 (*s*); 157.94 (*s*); 158.00 (*s*); 160.14 (*s*); 163.79 (*s*); 164.29 (*s*). FAB-MS: 533 (2, M^+), 429 (6), 413 (8), 392 (17), 391 (62), 338 (8), 309 (6), 279 (14), 225 (5), 177 (11), 155 (27), 153 (14), 152 (10), 135 (27), 133 (18), 121 (15), 119 (64), 113 (21), 105 (11), 103 (45).

Methyl 5-{{[5-Nitro-3-(1',2',3',4'-tetrahydro-2',4'-dioxopyrimidin-1'-yl)-2-thienyl]carbonyl}amino}-3-(1,2,3,4-tetrahydro-2,4-dioxopyrimidin-1-yl)thiophene-2-carboxylate (**15**). To a suspension of **12** (411 mg, 1.54 mmol), **8** (436 mg, 1.54 mmol) and anh. LiCl (1.63 g, 38.50 mmol) in THF (42 ml), DCC (540 mg, 2.62 mmol) in THF (5 ml) was added. The mixture was stirred vigorously under Ar for 2.5 h and then evaporated. The orange residue was resuspended in H_2O (50 ml) and stirred. The resulting red precipitate was filtered off and air-dried. This crude material was vigorously triturated with EtOH (40 ml) for 5 min, filtered off, and dried *in vacuo*: **15** (541 mg, 66%). Red powder. TLC (MeOH/CH_2Cl_2/Et_3N 1:9:0.05): R_f 0.20. UV/VIS (dioxane/H_2O 4:1): 268 (21400), 356 (13100), 456 (7400). IR (KBr): 3440*s*, 3220*m*, 3100*m*, 3050*m*, 2960*m*, 2856*m*, 1703*s*, 1575*m*, 1527*m*, 1461*m*, 1440*m*, 1420*m*, 1380*m*, 1343*m*, 1289*s*, 1200*w*, 1122*w*, 1092*m*, 1026*w*, 996*w*, 864*w*, 818*m*, 764*w*, 722*w*, 671*w*, 596*w*, 552*w*. ^{1}H-NMR (for numbering, see *Fig. 5*): 3.73 (*s*, MeOCO–C(2')(y^2)); 5.65 (*dd*, J = 7.9, 2.0, H–C(5)(y^2)); 5.76 (*dd*, J = 8.1, 2.2, H–C(5)(y^1)); 7.03 (*s*, H–C(4')(y^2)); 7.60 (*d*, J = 7.7, H–C(6)(y^2)); 7.81 (*d*, J = 8.1, H–C(6)(y^1)); 8.42 (*s*, H–C(4')(y^1)); 11.46 (*d*, J = 1.8, H–N(3)(y^2)); 11.63 (*d*, J = 1.8, H–N(3)(y^1)); 12.82 (*s*, NH–C(5')(y^2)). ^{13}C-NMR (for numbering, see *Fig. 5*): 52.23 (*q*, MeOCO–C(2')(y^2)); 101.30 (*d*, C(5)(y^2)); 102.27 (*d*, C(5)(y^1)); 114.59 (*d*, C(4')(y^2)); 116.37 (*s*); 129.28 (*d*, C(4')(y^1)); 133.50 (*s*); 136.18 (*s*); 139.15 (*s*); 142.74 (*s*); 144.80 (*d*, C(6)(y^2)); 145.72 (*d*, C(6)(y^1)); 149.92 (*s*); 149.96 (*s*); 150.07 (*s*); 156.83 (*s*); 160.75 (*s*); 163.59 (*s*); 163.94 (*s*). EI-MS: 532 (1, M^+), 447 (1), 389 (1), 346 (1), 295 (5), 281 (12), 280 (9), 268 (5), 267 (25), 266 (33), 239 (22), 224 (10), 209 (9), 197 (7), 196 (38), 193 (10), 166 (5), 149 (6), 138 (10), 137 (5), 122 (17), 112 (68), 101 (11), 99 (10), 95 (7), 86 (39), 70 (12), 69 (23), 60 (11), 58 (13), 44 (100).

REFERENCES

[1] G. Sauter, 'Design, Synthese und Eigenschaften eines DNA-Analogons mit Polyamidrückgrat ('Distamycin-NA')', Inauguraldissertation, Universität Bern, 1997.

[2] A. De Mesmaeker, R. Häner, P. Martin, H. E. Moser, *Acc. Chem. Res.* **1995**, *28*, 366; 'Methods in Molecular Medicine™', 'Antisense Therapeutics', Ed. S. Agrawal, Humana Press, Totowa, New Jersey, 1996.

[3] P. E. Nielsen, M. Egholm, R. H. Berg, O. Buchardt, *Science (Washington D.C.)* **1991**, *254*, 1497.

[4] M. Egholm, O. Buchardt, L. Christensen, C. Behrens, S. Freier, D. A. Driver, R. H. Berg, S. K. Kim, B. Norden, P. E. Nielsen, *Nature (London)* **1993**, *365*, 566.

[5] M. L. Kopka, C. Yoon, D. Goodsell, P. Pjura, R. E. Dickerson, *Proc. Natl. Acad. Sci. U.S.A.* **1985**, *82*, 1376; M. Coll, C. A. Frederick, A. H.-J. Wang, A. Rich, *ibid.* **1987**, *84*, 8385; C. Zimmer, *Prog. Nucl. Acid Res. Mol. Biol.* **1975**, *15*, 285; C. Zimmer, U. Wahnert, *Prog. Biophys. Mol. Biol.* **1986**, *47*, 31.

[6] R. S. Youngquist, P. B. Dervan, *J. Am. Chem. Soc.* **1987**, *109*, 7564.

[7] J. W. Trauger, E. E. Baird, P. B. Dervan, *Nature (London)* **1996**, *382*, 559.

[8] P. Rossy, F. Vogel, to *BASF*, Pat. DE 3018134 A1, C 07 D 333/38, 1981; P. Rossy, F. Vogel, W. Hoffmann, J. Paust, A. Nürrenbach, *Tetrahedron Lett.* **1981**, *22*, 3493.
[9] G. Shaw, R. N. Warrener, *J. Chem. Soc.* **1958**, 153; G. Shaw, R. N. Warrener, *ibid.* **1958**, 157.
[10] Y. F. Shealy, C. Allen O'Dell, M. C. Thorpe, *J. Heterocycl. Chem.* **1981**, *18*, 383.
[11] R. L. Elliott, P. J. O'Hanlon, N. H. Rogers, *Tetrahedron* **1987**, *43*, 3295.
[12] P. K. Kadaba, *Synthesis* **1972**, 628.
[13] 'The Chemistry of Heterocyclic Compounds', Series Ed. E. C. Taylor, 'Thiophene and Its Derivatives', Vol. Ed. S. Gronowitz, John Wiley & Sons, Inc., New York 1991, Vol. 44, Part 4, p. 31; F. Mathieu, *Acta Crystallogr., Sect. B* **1980**, *36*, 2715.
[14] W. Saenger, 'Principles of Nucleic Acid Structure', Ed. C. R. Cantor, Springer Verlag, New York, 1984, p. 51, p. 122.
[15] N. Zinin, *J. Prakt. Chem.* **1842**, *27*, 149. T. E. Nickson, *J. Org. Chem.* **1986**, *51*, 3903; H. K. Porter, in 'Organic Reactions', Ed. W. G. Dauben, John Wiley, New York, 1973, Vol. 20, p. 455; D. A. Burgess, I. D. Rae, *Aust. J. Chem.* **1977**, *30*, 927.
[16] D. Seebach, A. K. Beck, A. Studer, 'Modern Synthetic Methods 1995', Eds. B. Ernst and C. Leumann, Verlag Helvetica Chimica Acta, Basel, 1995, pp. 3–178.
[17] M. Hesse, H. Meier, B. Zeeh, 'Spektroskopische Methoden in der organischen Chemie', Georg Thieme Verlag, Stuttgart' 1987, p. 94.
[18] S. Içli, *Org. Magn. Reson.* **1979**, *12*, 178.
[19] M. J. S. Dewar, E. G. Zoebisch, E. F. Healy, J. J. P. Stewart, *J. Am. Chem. Soc.* **1985**, *107*, 3902; J. J. P. Stewart, *J. Comput. Chem.* **1980**, *10*, 209.
[20] R. Gallo, C. Roussel, U. Berg, in 'Advances in Heterocyclic Chemistry', Ed. A. R. Katritzky, Academic Press, Inc., London, 1988, Vol. 43, pp. 239–271.
[21] R. Hirsenkorn, R. R. Schmidt, *Liebigs Ann. Chem.* **1990**, 883; L. F. Tietze, C. Schneider, M. Pretor, *Synthesis* **1993**, 1079.
[22] G. M. Sheldrick, 'SHELXTL PC, Structure Determination Software', Siemens Analytical X-Ray Instruments Inc., Madison, Wisconsin, USA, 1990.
[23] G. M. Sheldrick, 'SHELXL93, Program for Crystal Structure Determination' University of Goettingen, Federal Republic of Germany 1993.

Received September 8, 1997